

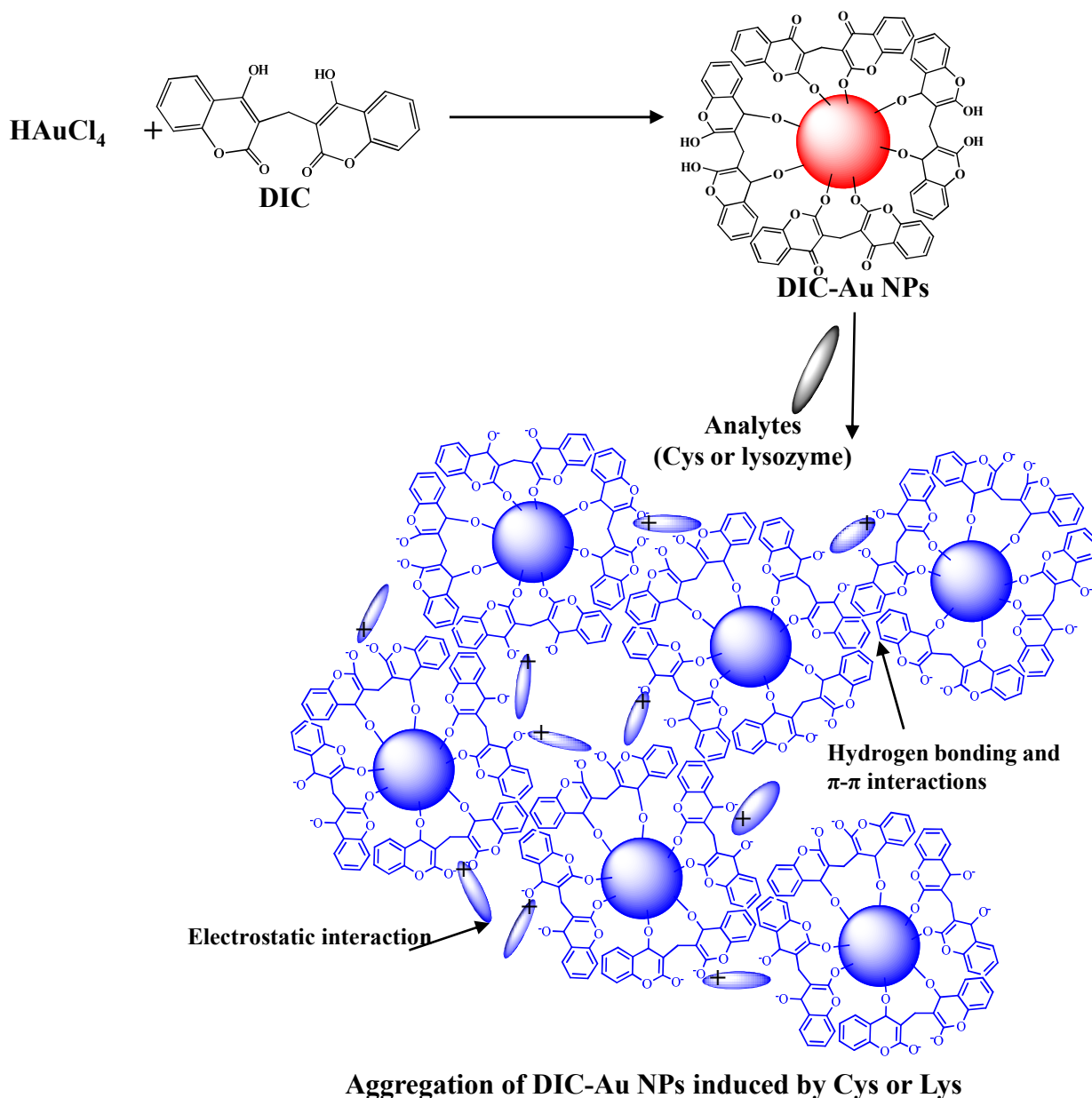
Supporting Information of
Dicoumarol assisted synthesis of water dispersible gold nanoparticles for colorimetric sensing of
cysteine and lysozyme in biofluids

Betha Saineelima B. Kasibabu, Jigna R. Bhamore, Stephanie L. D'souza and Suresh Kumar Kailasa*

Department of Applied Chemistry, S. V. National Institute of Technology, Surat-395 007, India

*Corresponding author; Phone: +91-261-2201730; Fax: +91-261-2227334

E-mail: sureshkumarchem@gmail.com; skk@ashd.svnit.ac.in



Scheme S1. A schematic representation of the mechanism for the colorimetric sensing Cys and Lys using DIC-Au NPs as a probe.

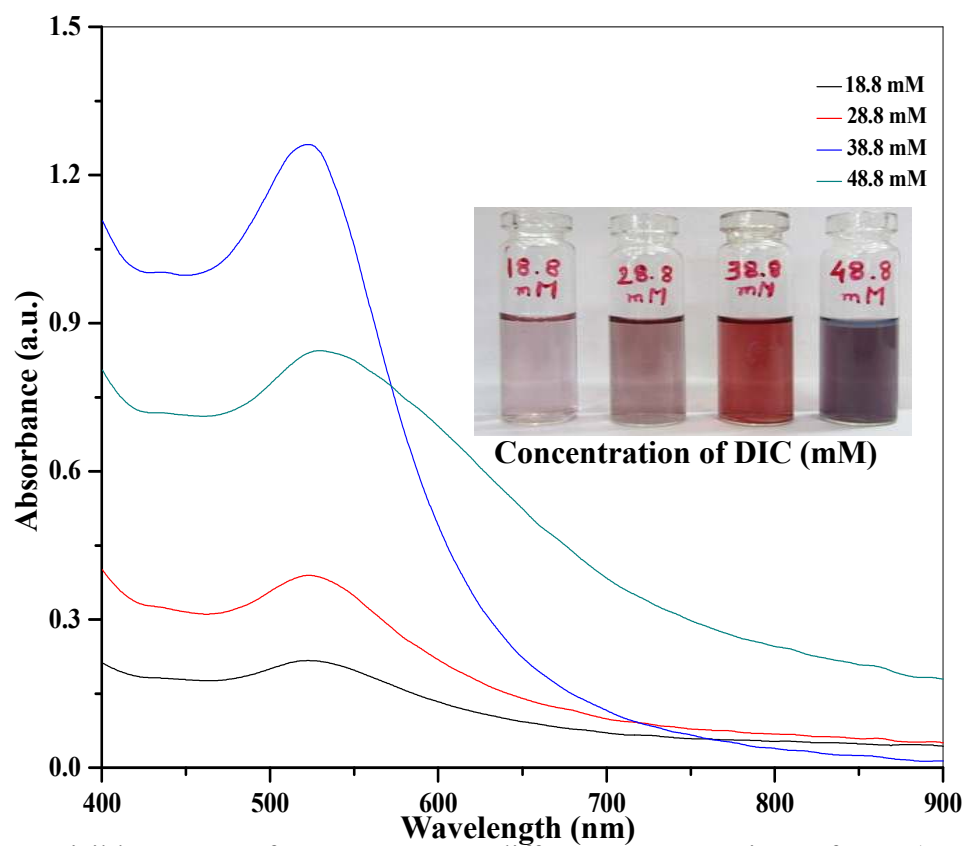


Figure S1. UV-visible spectra of DIC-Au NPs at different concentrations of DIC (18.8 – 48.8 mM). Inset: Photographic image of corresponding solutions.

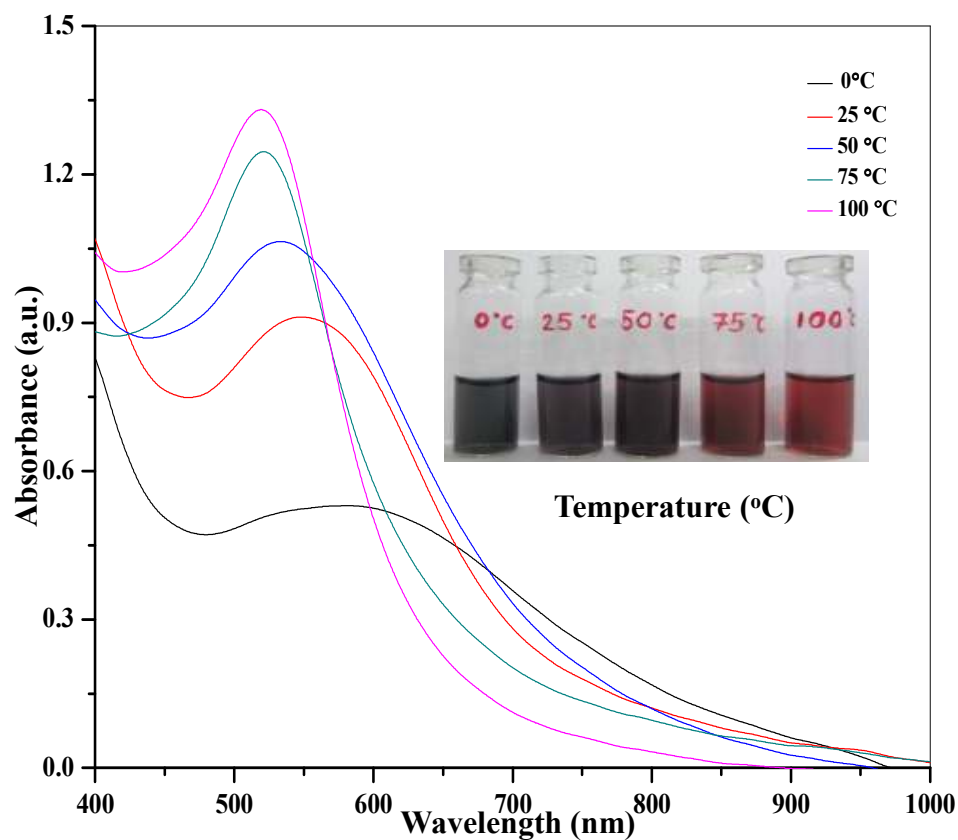


Figure S2. UV-visible spectra of DIC-Au NPs at different temperature (0 – 100°C). Inset: Photographic image of DIC-Au NPs at different temperature.

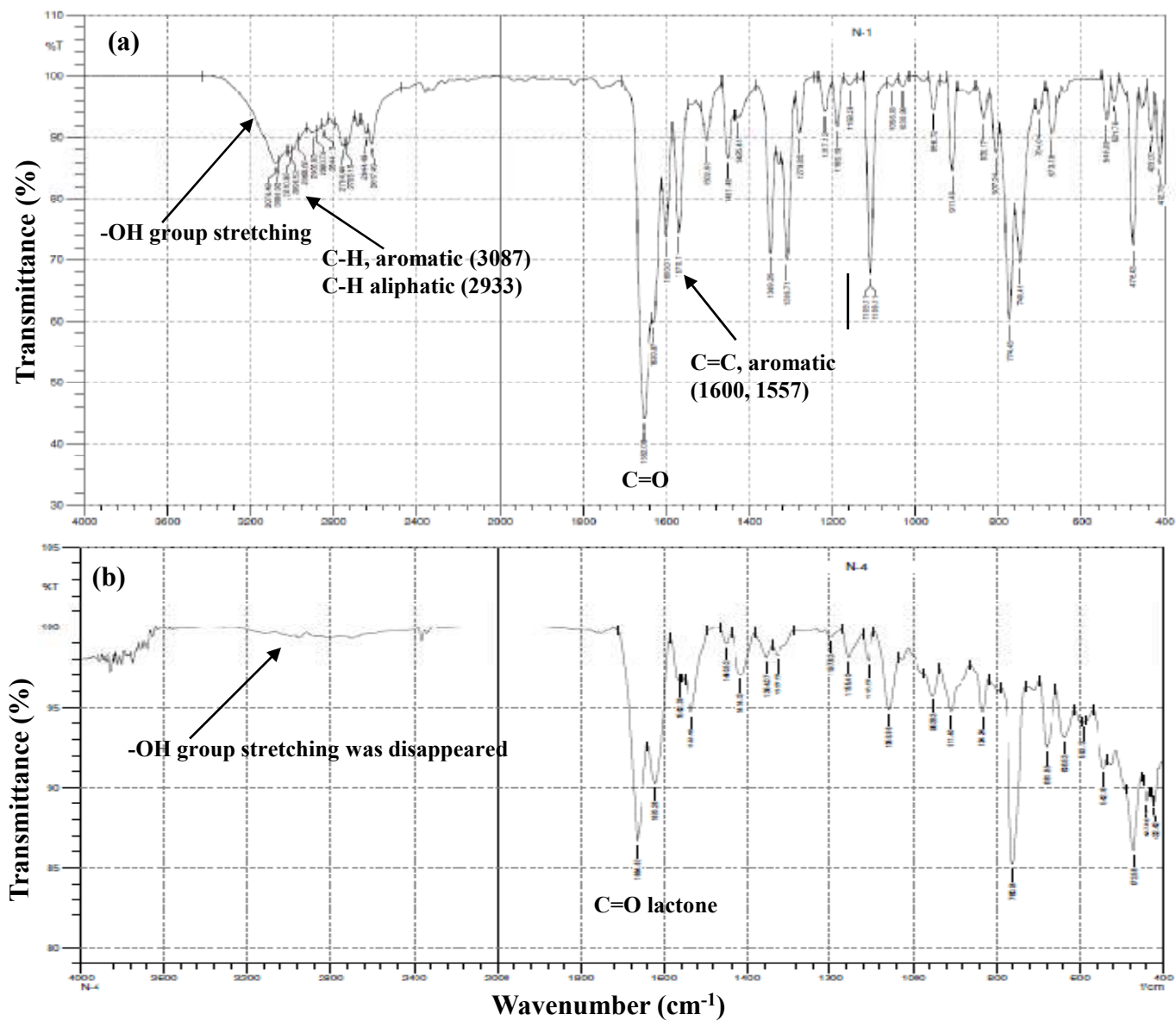


Figure S3. FT-IR spectra of (a) pure DIC and (b) DIC-Au NPs.

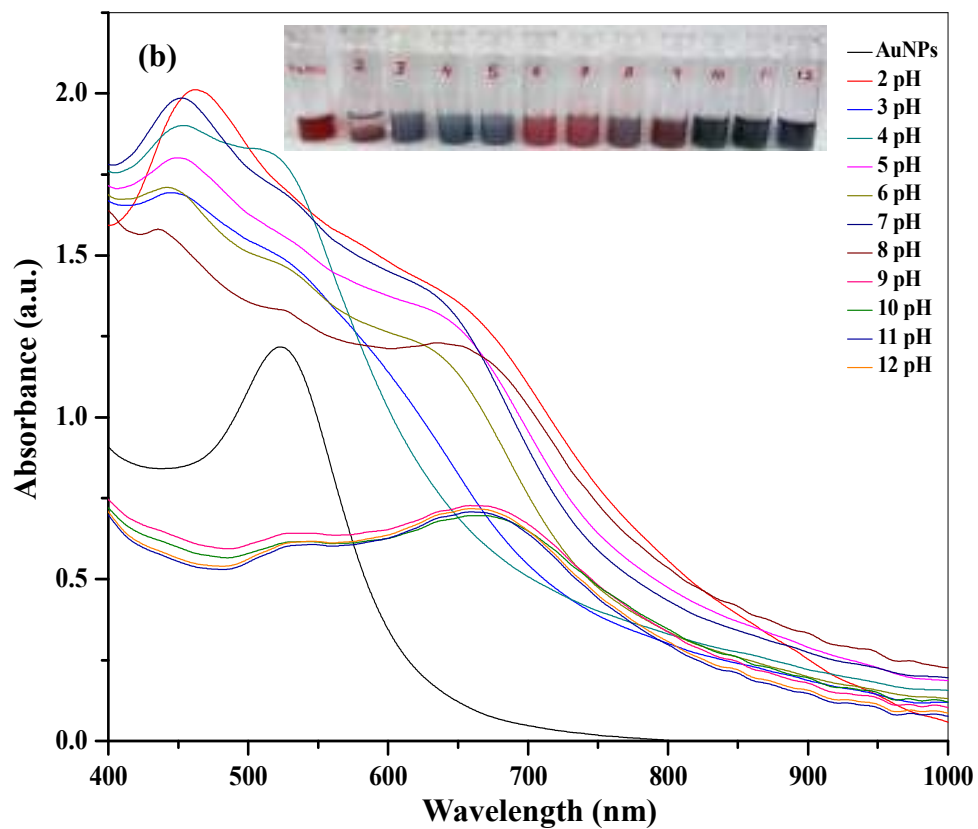
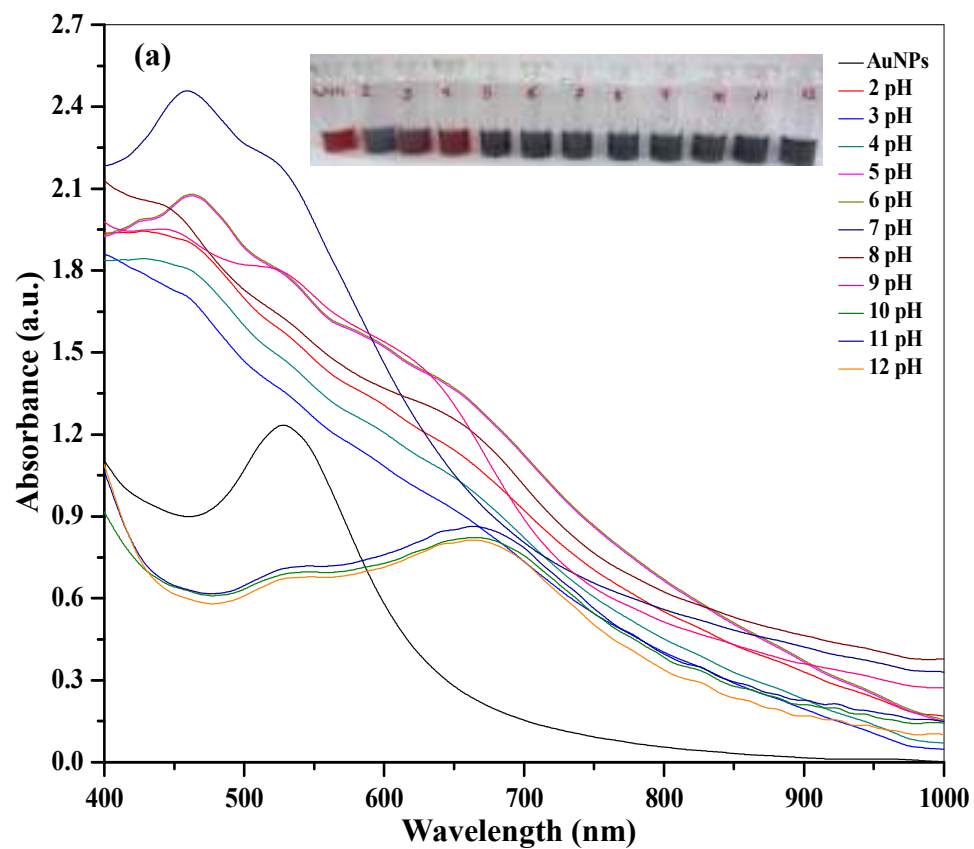


Figure S4. (a) UV-visible spectra of DIC-Au NPs in the presence of Cys (1 mM) at ammonium acetate pHs from 2.0 to 12.0. Inset: Photographic image of corresponding solutions. (b) UV-visible spectra of DIC-Au NPs in the presence of Cys (1 mM) at PBS pHs from 2.0 to 12.0. Inset: Photographic image of corresponding solutions.

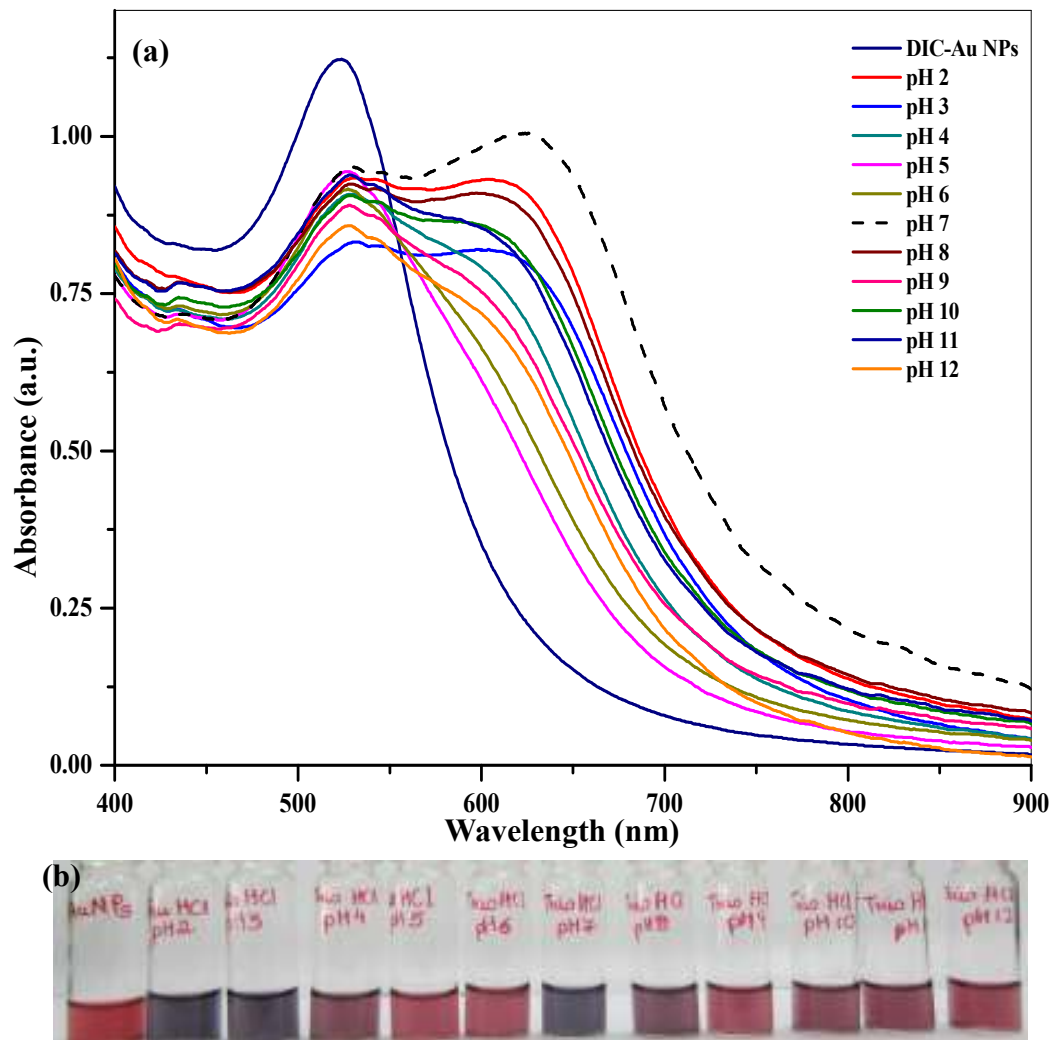


Figure S5. (a) UV-visible spectra of DIC-Au NPs in the presence of Cys (1 mM) at Tris-HCl pHs from 2.0- to 12.0. (b) Photographic image of corresponding solutions.

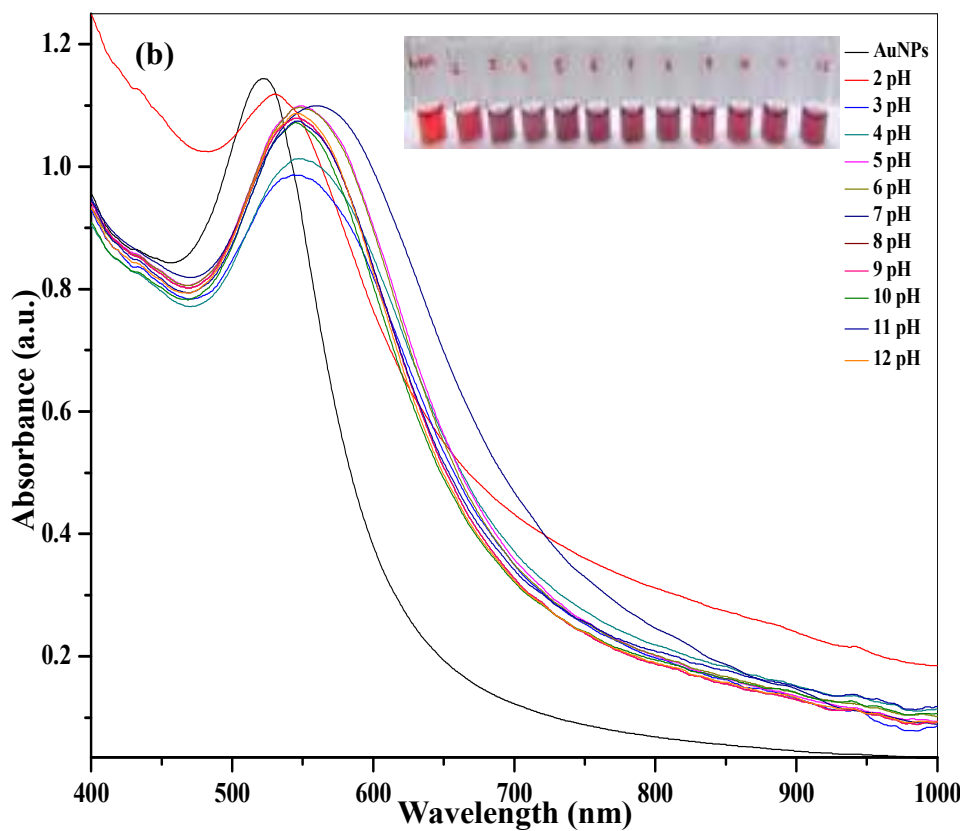
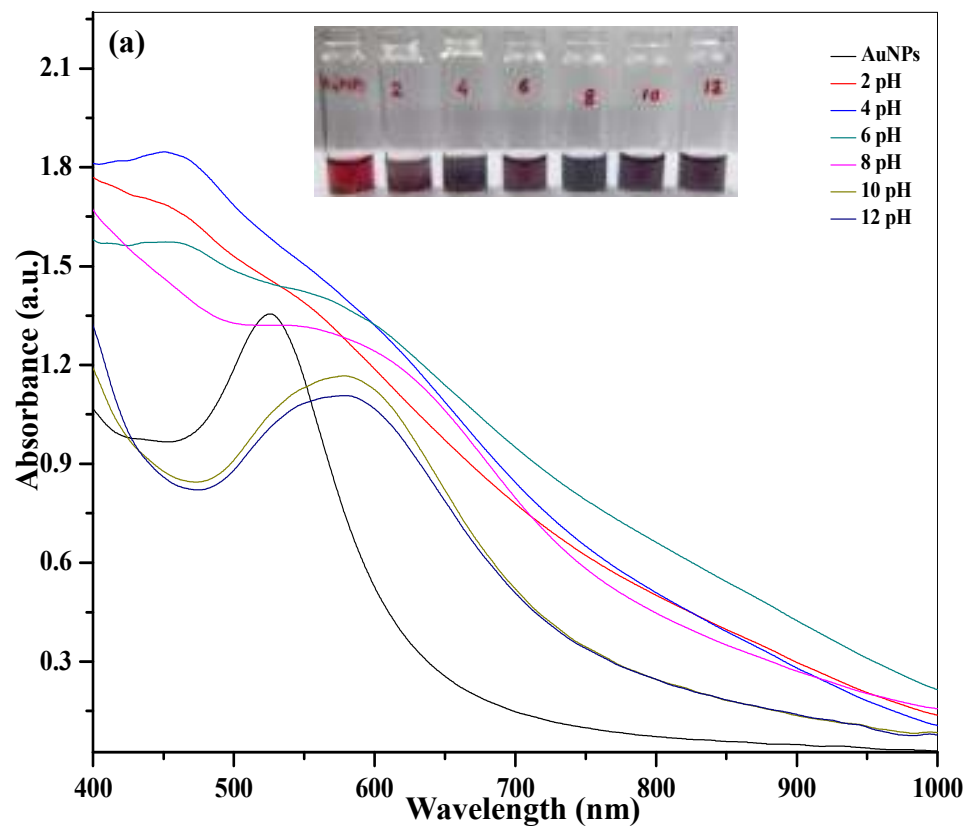


Figure S6. (a) UV-visible spectra of DIC-Au NPs in the presence of Lys (50 μM) at ammonium acetate pHs from 2.0 to 12.0. Inset: Photographic image of corresponding solutions. (b) UV-visible spectra of DIC-Au NPs in the presence of Lys (50 μM) at PBS pHs from 2.0 to 12.0. (c) Photographic image of corresponding solutions.

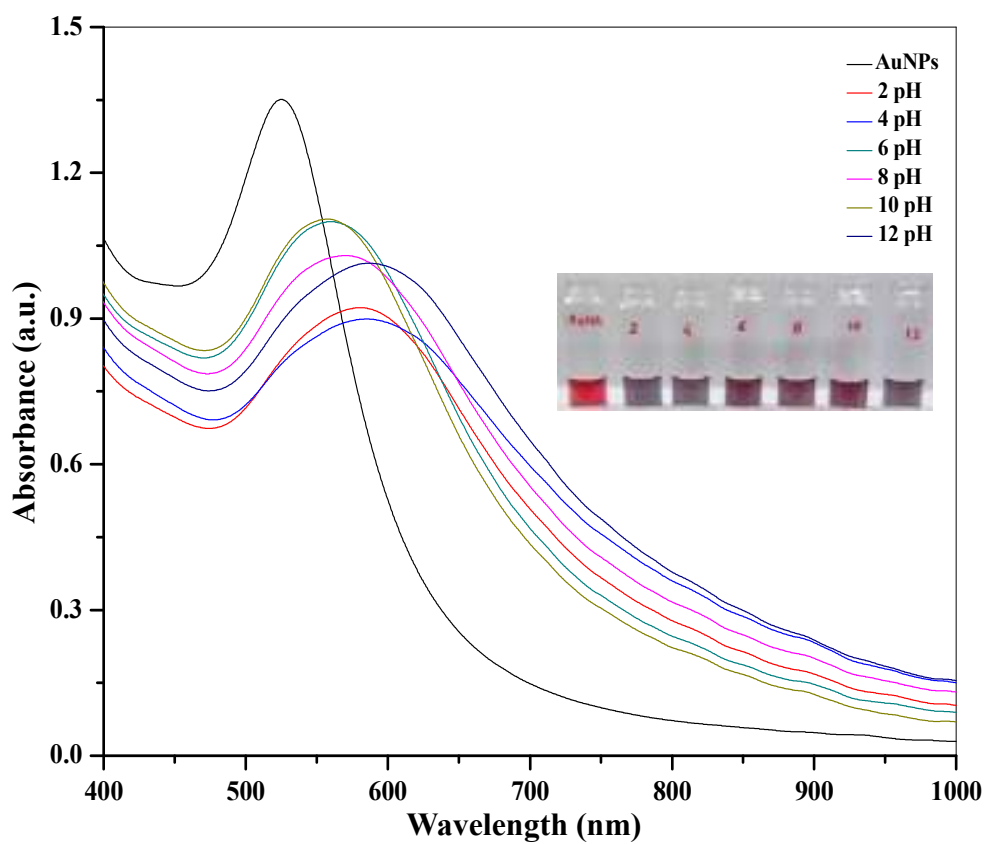


Figure S7. UV-visible spectra of DIC-Au NPs in the presence of Lys (50 μ M) at Tris-HCl pH from 2.0 to 12.0. Inset: Photographic image of corresponding solutions.

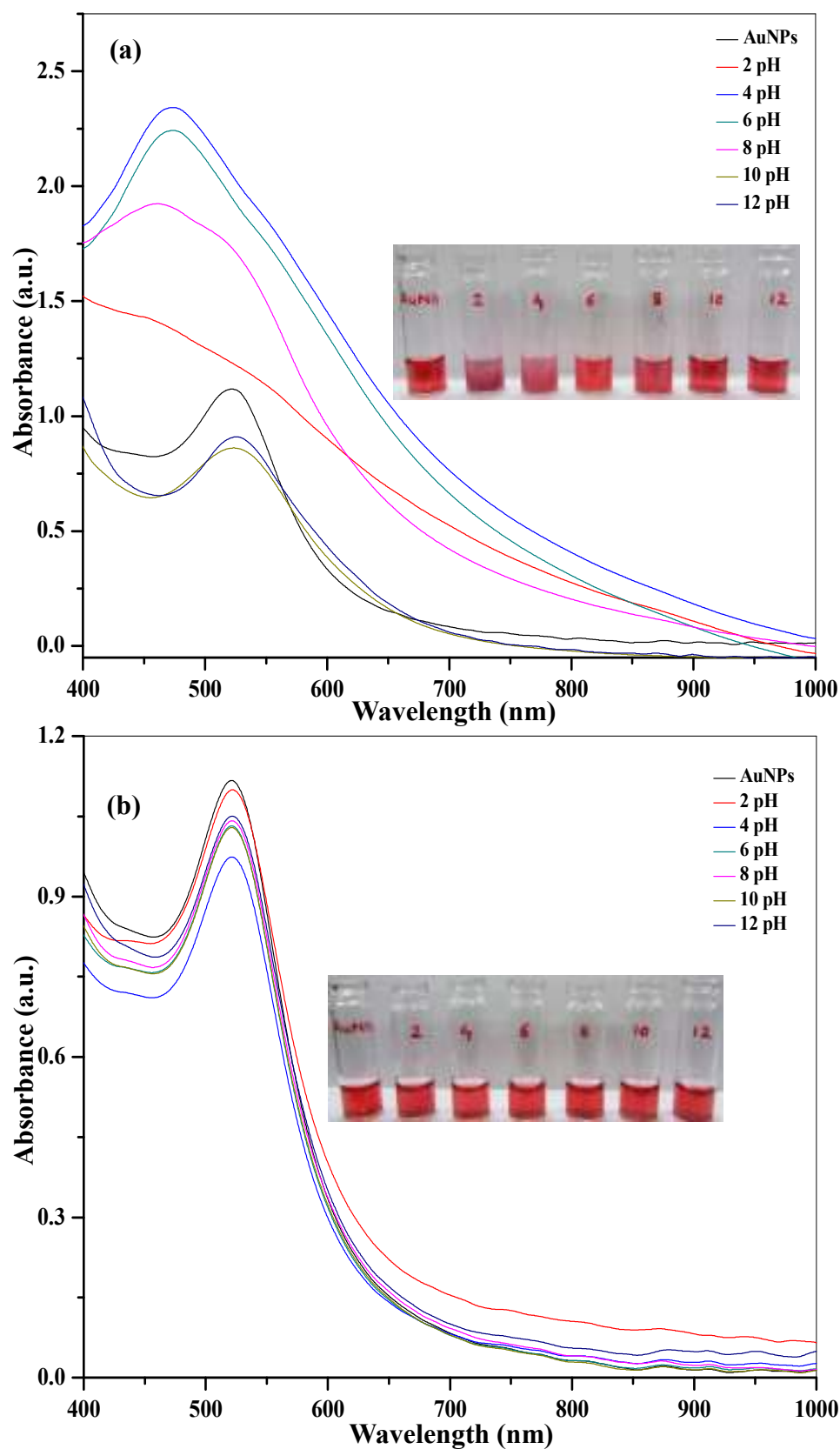


Figure S8. (a) UV-visible spectra of DIC-Au NPs in the presence of ammonium acetate buffer in pH range from 2.0 to 12.0 without analytes. Inset: Photograph of corresponding solutions. (b) UV-visible spectra of DIC-Au NPs in the presence of PBS in pH range from 2.0 to 12.0. Inset: Photograph of corresponding solutions.

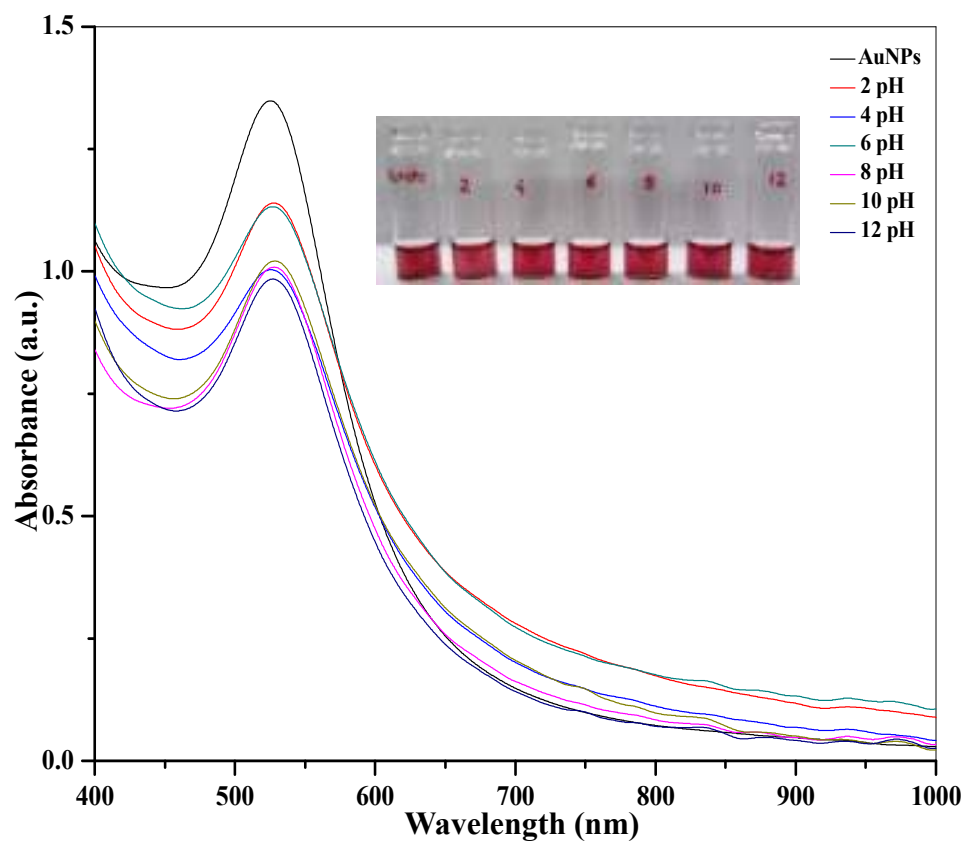


Figure S9. UV-visible spectra of DIC-Au NPs in the presence of Tris-HCl buffer in pH range from 2.0 to 12.0 without analytes. Inset: Photograph of corresponding solutions.

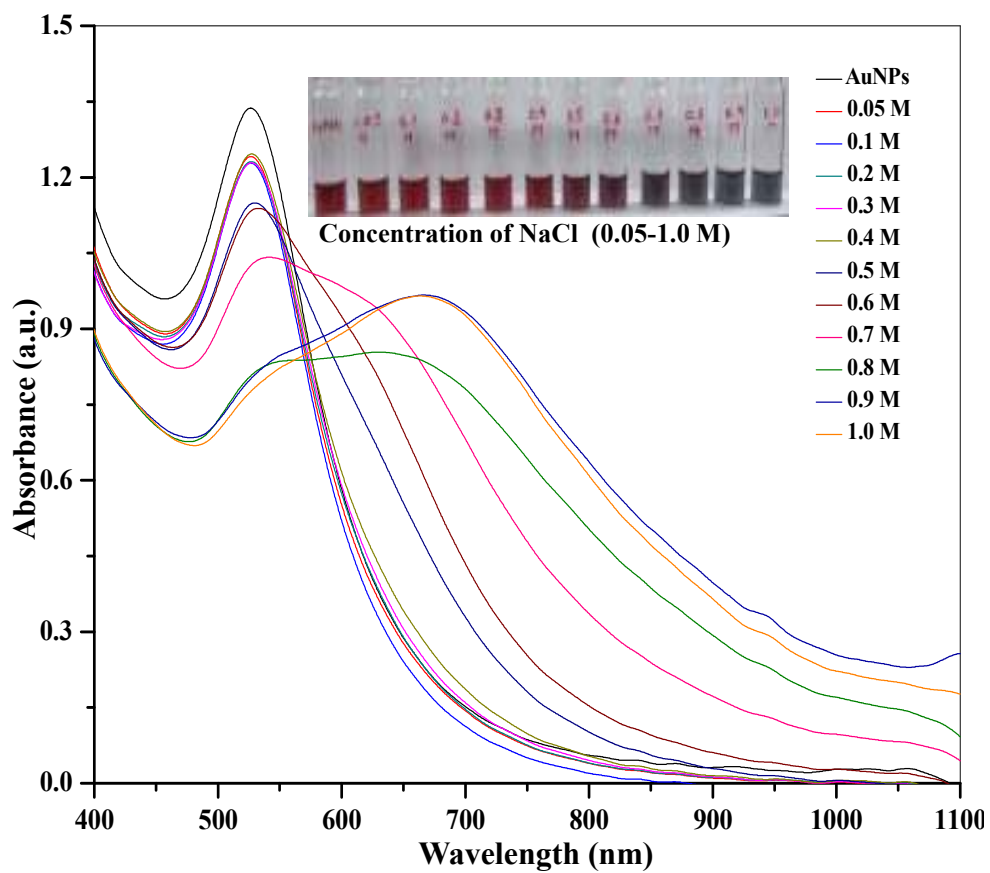


Figure S10. UV-visible spectra of DIC-Au NPs by the addition of NaCl from 0.05 to 1.0 M without target analytes. Inset images are the corresponding photographs of Au NPs color.

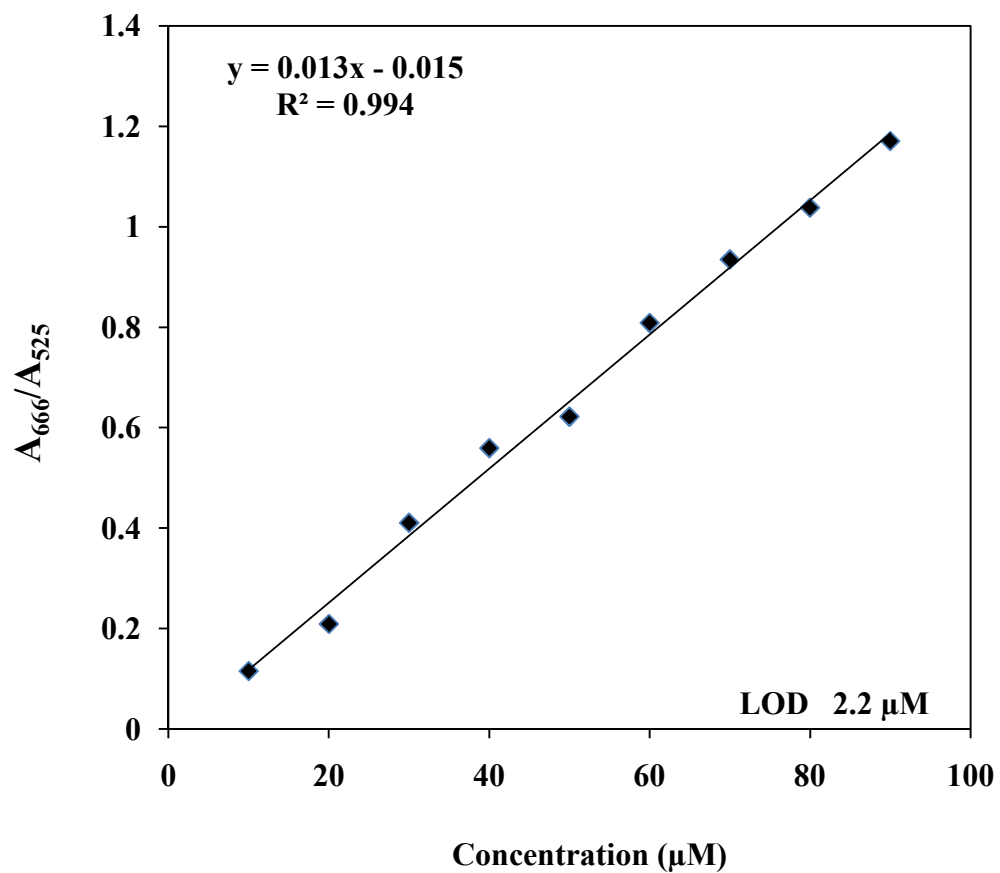


Figure S11. Calibration graph for the detection of Cys in the concentration range of 10-90 μM using DIC-Au NPs as a probe at absorption ratio at A_{666}/A_{525} versus Cys concentration.

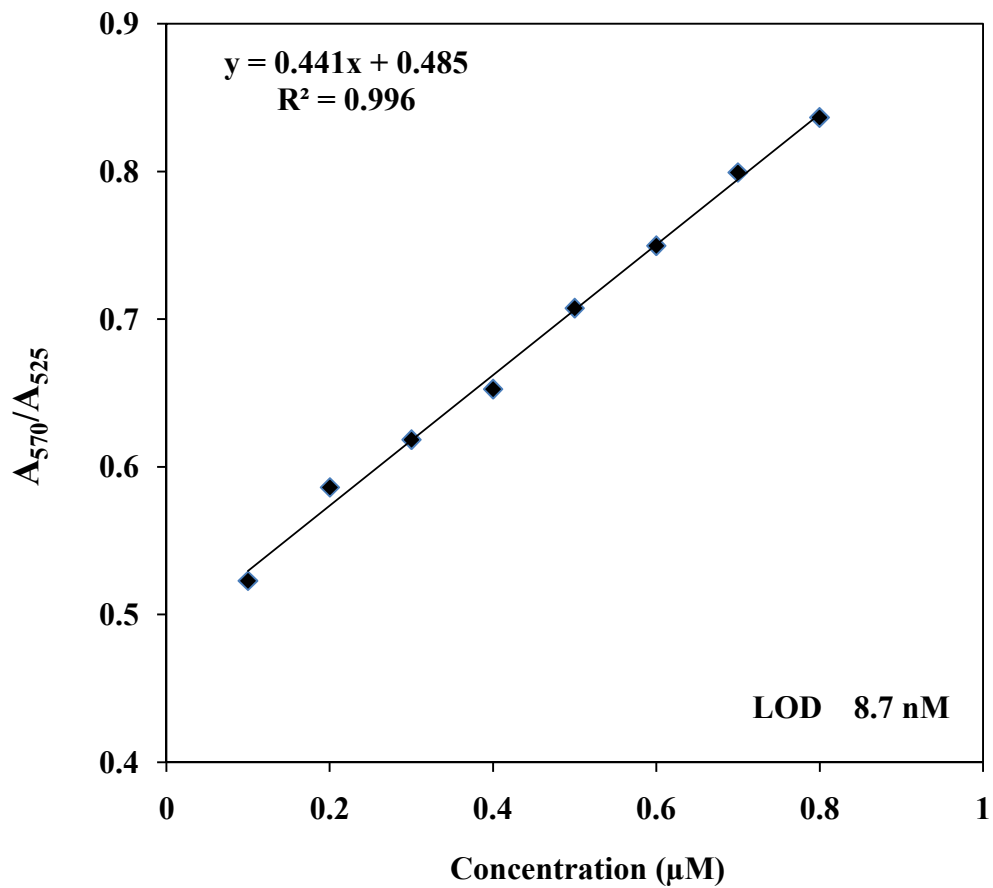


Figure S12. Calibration graph for the detection of Lys in the concentration range of 100-800 nM using DIC-Au NPs as a probe at absorption ratio at A_{570}/A_{525} versus Lys concentration.

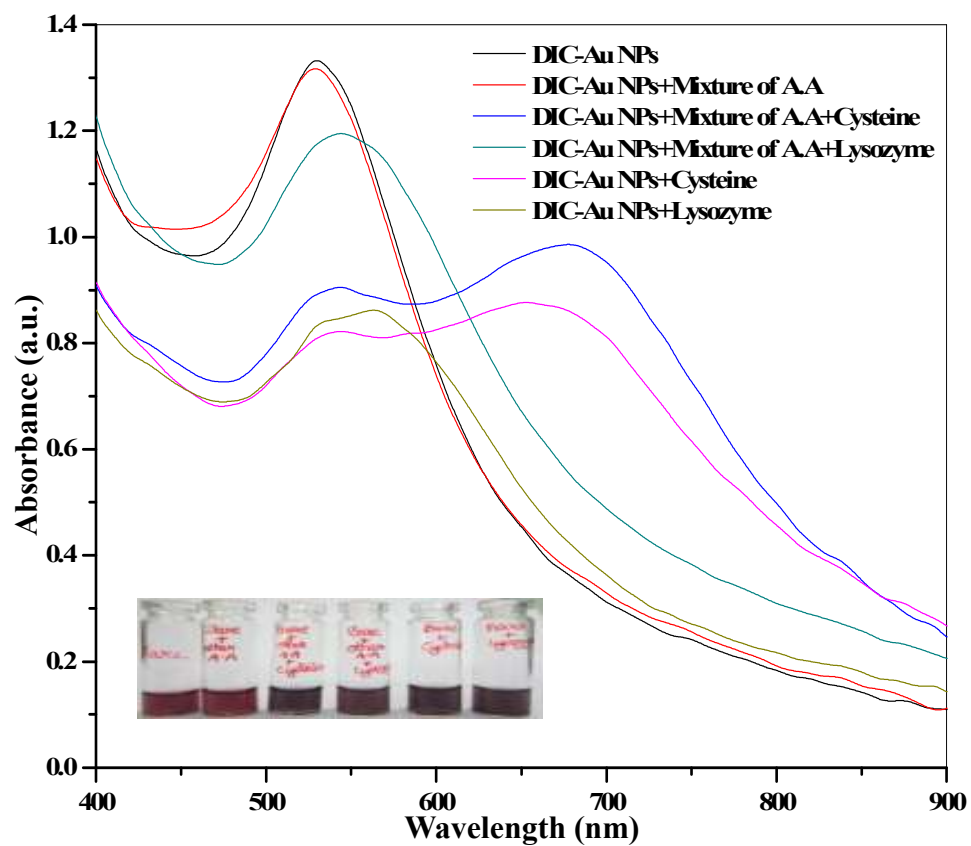


Figure S13. UV-visible absorbance spectra of DIC-Au NPs in the presence of various aminoacids (phenyl alanine, histidine, 4-hydroxyproline, proline, tryptophan, tyrosine, alanine, isoleucine, asparagine, aspartic acid, methionine, lysine, serine and leucine, 1 mM) for detection of Cys and Lys. Inset: the corresponding photographic image.

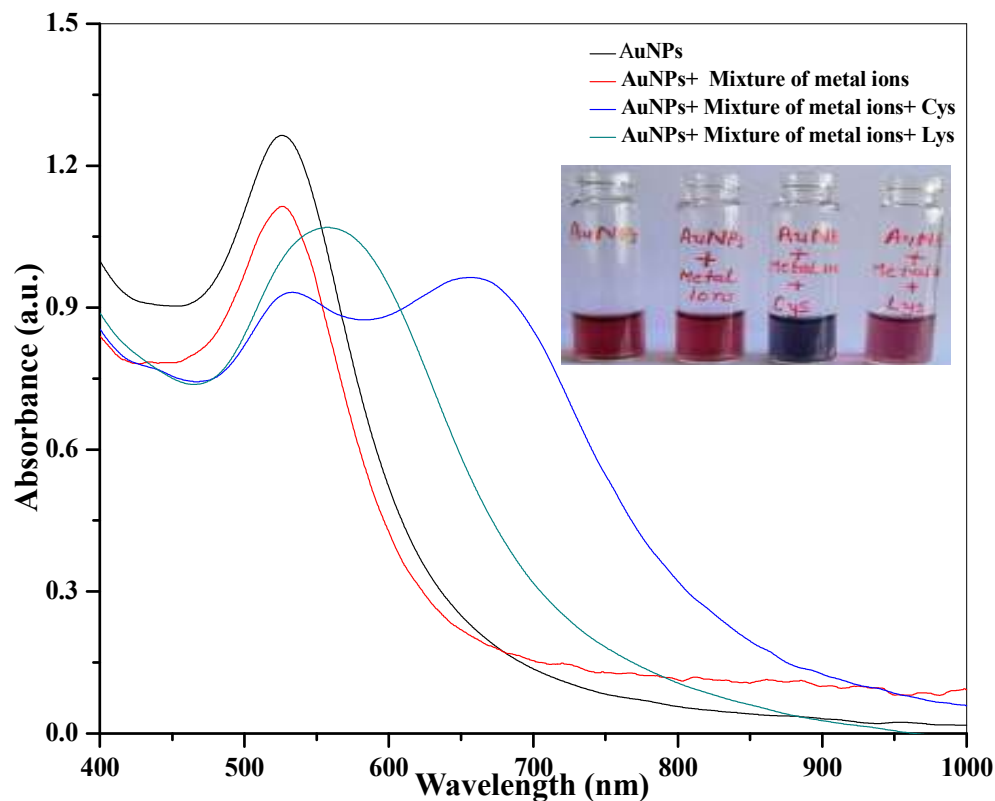


Figure S14. UV-visible absorbance spectra of DIC-Au NPs in the presence of Cys and Lys upon addition of various metal ions (Na^+ , K^+ , Br^{2+} , Ca^{2+} , Cu^{2+} , Zn^{2+} , Ni^{2+} , Fe^{2+} , Fe^{3+} and Al^{3+} , 1.0 mM). Inset: the corresponding photographic image.

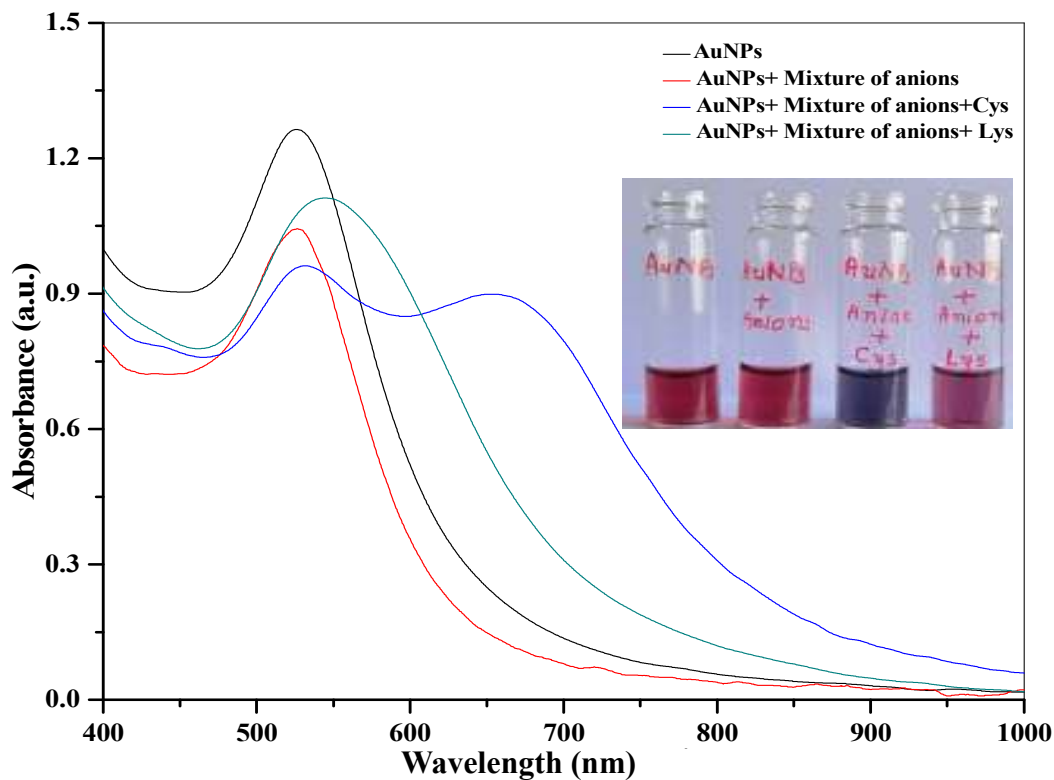


Figure S15. UV-visible absorbance spectra of DIC-Au NPs in the presence of Cys and Lys upon addition of various anions (Cl^- , Br^- , I^- , F^- , SO_4^{2-} , S^{2-} , PO_4^{3-} and $\text{Cr}_2\text{O}_7^{2-}$, 1.0 mM). Inset: the corresponding photographic image.

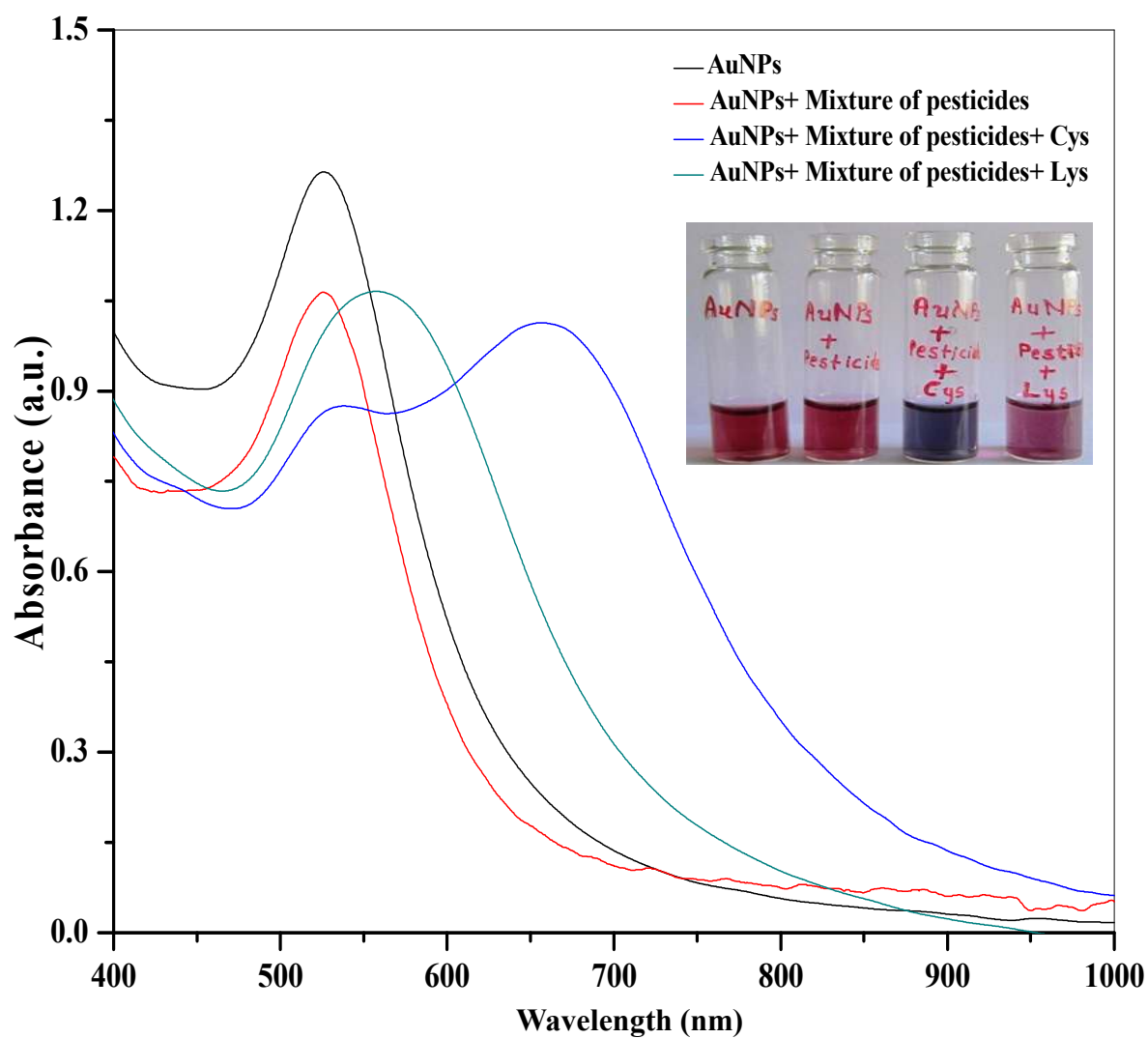


Figure S16. UV-visible absorbance spectra of DIC-Au NPs in the presence of Cys and Lys upon addition of various pesticides (chlorpyrifos, quinalphos, hexaconazole, tricyclazole, acephate, metsulfuron, isoproturon, and chlopropham, 1.0 mM). Inset: the corresponding photographic image.

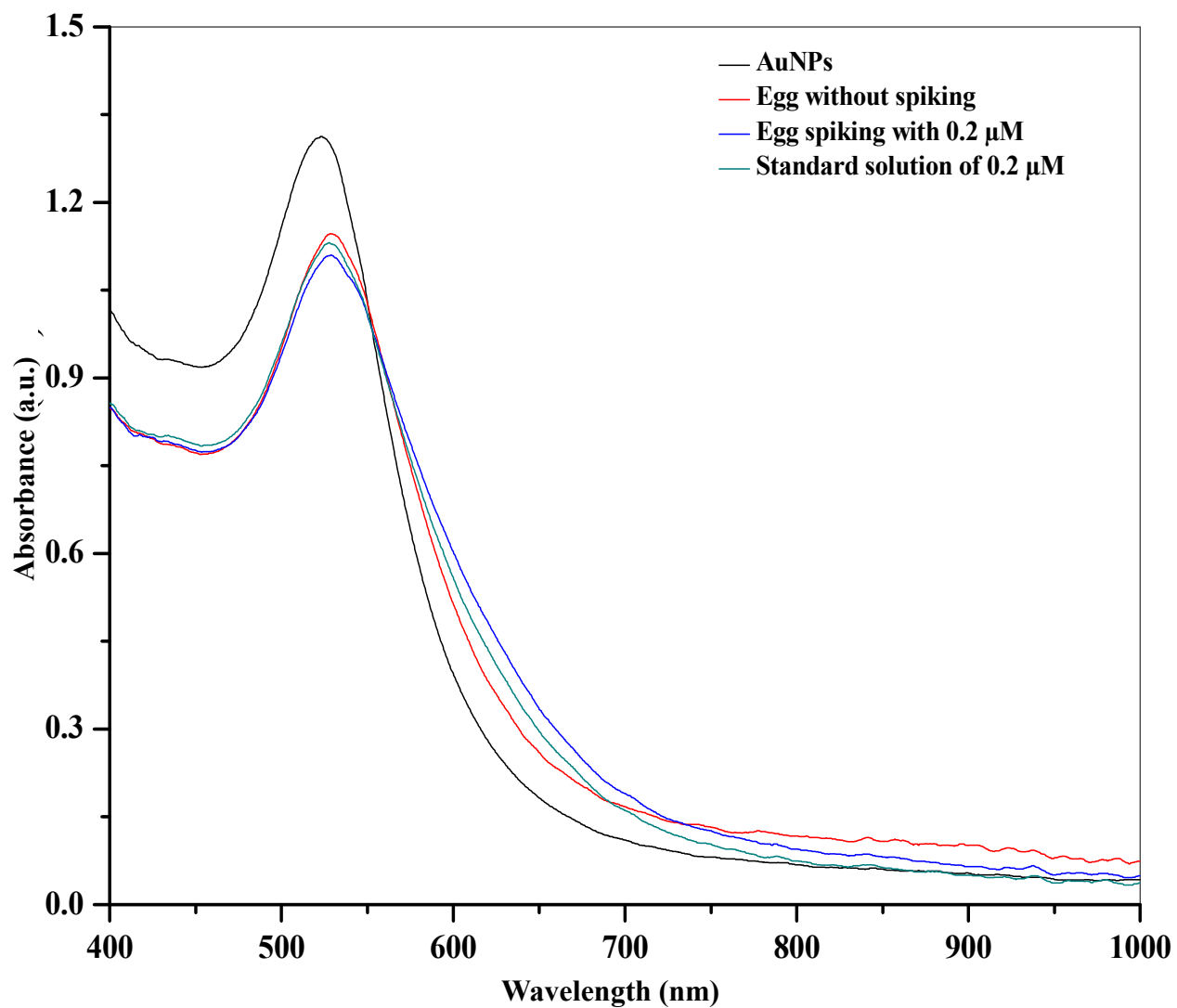


Figure S17. UV-visible spectral variations of DIC-Au NPs in egg white (without spiking of Lys), and with spiking 0.2 μM of Lys and the spectrum of DIC-Au NPs in the presence of standard Lys at PBS pH 7.

Table S1. Analysis of Cys and Lys in biological samples using DIC-Au NPs as a probe.

Sample	Cys				Lys			
	Added ^a	Found ^a	Recovery (%) ^b	RSD	Added ^a	Found ^a	Recovery (%) ^b	RSD
Urine 1	40	39.8	99.5	0.28	0.2	0.21	104.8	2.2
	60	59.9	99.8	0.18	0.5	0.52	104.0	2.9
	80	78.0	97.5	1.82	0.8	0.81	102.2	2.2
Urine 2	40	39.1	97.8	0.12	0.2	0.19	98.6	2.7
	60	57.6	96.0	0.38	0.5	0.51	101.0	2.1
	80	77.8	97.3	0.98	0.8	0.81	100.8	1.6
Urine 3	40	41.2	103.2	0.23	0.2	0.20	101.3	0.7
	60	63.7	106.2	0.18	0.5	0.49	99.4	1.1
	80	85.2	106.5	0.42	0.8	0.81	101.3	1.3
Plasma 1	40	42.2	105.7	0.45	0.2	0.19	97.2	0.3
	60	65.0	108.3	0.14	0.5	0.47	95.1	1.8
	80	85.8	107.2	1.79	0.8	0.75	94.3	1.8
Plasma 2	40	39.1	97.8	0.10	0.2	0.19	95.3	2.6
	60	58.9	98.3	0.11	0.5	0.49	98.9	1.3
	80	78.1	97.6	1.80	0.8	0.77	96.0	1.8
Plasma 3	40	39.1	97.7	0.44	0.2	0.21	102.0	0.9
	60	57.5	95.9	0.14	0.5	0.50	100.2	1.5
	80	77.3	96.6	0.93	0.8	0.79	99.15	2.3
Egg white	-	-	-	-	0.2	0.22	108.4	2.5
	-	-	-	-	0.5	0.55	110.6	2.0
	-	-	-	-	0.8	0.86	108.5	2.6

^aμM, ^bn=3